Research Report

2014-29

Dual-Stator Interior Permanent Magnet Vernier Machine for Torque Density and Power Factor Improvement

F. Zhao, T.A. Lipo*, B. Kwon

Department of Electronic Systems Engineering,
Hanyang University,
Ansan-si, Gyeonggi-do, 426-791, Korea

* Department of Electrical and Computer Engineering,
University of Wisconsin-Madison,
Madison, WI, 53706-1691, USA

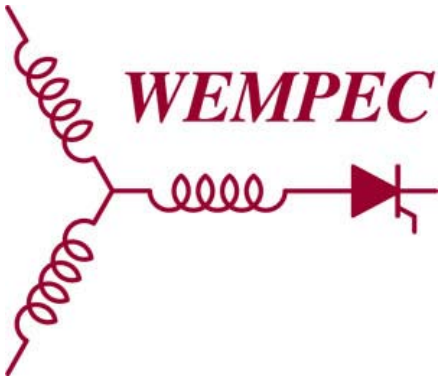

Wisconsin
Electric
Machines &
Power
Electronics
Consortium

University of Wisconsin-Madison
College of Engineering
Wisconsin Power Electronics Research Center
2559D Engineering Hall
1415 Engineering Drive
Madison WI 53706-1691

Electric Power Components and Systems,

Dual-Stator Interior Permanent Magnet Vernier Machine for Torque Density and Power Factor Improvement

Fei Zhao[1], Thomas A. Lipo[2] and Byung-il Kwon[1]

[1]Department of Electronic Systems Engineering, Hanyang University, Ansan, Korea
[2]Department of Electrical and Computer Engineering, University of Wisconsin-Madison, Madison, Wisconsin, USA

Abstract *An improved topology of a low-speed permanent magnet vernier machine called a dual-stator interior permanent magnet vernier machine (DS-IPMVM) is introduced to significantly increase torque density and power factor. Dual-stator is usually adopted in machine design for more torque and the abundant space utilization. Interior spoke-type magnet array in the rotor is designed for magnet flux focusing, which can effectively increase useful flux and force flux lines pass through the entire machine during operation other than two separate torque components as in a normal dual-stator PM machines. In order to clearly place the advantages of the proposed topology in perspective, the proposed DS-IPMVM is compared to a well-known dual-stator surface-mounted permanent magnet vernier machine (DS-SPMVM). This article discusses the operation principle and magnetic field analysis of the proposed machine and reports the comparison simulation results taken from finite element method. In addition, the stator slot pitch is optimized for further better performance on torque density and power factor.*

Keywords AC machines, dual stator, finite element method (FEM), power factor, PMVM, torque density

1. Introduction

The permanent magnet vernier machine (PMVM) is regarded by now as a suitable alternative for low-speed direct-drive applications such as wind turbine generators, electrical vehicles motors, cooling tower motors and so on. The PMVM is a unique electromechanical device invented in Japan [1], which is derived from the earlier vernier reluctance machine [2]. The configuration of a much larger number of pole pairs than the number of stator winding pole pairs is designed in PMVM other than equal to the number of stator winding pole pairs in

Manuscript received **, 2013.
Address Correspondence to Byung-il Kwon, Department of Electronic Systems Engineering, Hanyang University, Ansan, Korea, 426791. Email: bikwon@hanyang.ac.kr.

a conventional PM machine. It can cause the so-called “magnetic gearing effect”, which is that a little movement of the rotor brings a huge flux change for a high steady torque generation [1]-[6]. Since PM vernier machine normally designed with a large magnet pole number, it suits to a relative low speed operation due to the phase voltage or bus voltage limitation. Thus, reduction gears with backlash are not necessary in a direct drive vernier machine system. Large pole pairs but low rated speed makes the operation frequency in PMVM not so high and the loss in steel cores will not be a big issue. Classical air cooling can be adopted for this low speed high torque machine.

One of the limitations associated with a vernier machine, however, is the undesirable feature of poor power factor, which calls for a high power rating requirement for the drive inverter. The same PM volume in a vernier machine is unable to achieve the same flux density value as in a normal PM machine. That is because PM arrangement corresponding one stator winding pole in a PMVM produces a heteropolar field, not all of the poles under one winding pole generate useful flux at any instant. Therefore, a larger reactive effect or a larger number of turns is needed for a given design, resulting in a poor power factor. If a PM vernier machine is designed with the same stator and winding as in a normal PM machine, the armature inductance can be assumed as the same in a reasonable design. In this case, the flux linkage in a vernier machine is lower and also a lower power factor will occur. The above points out that a poor power factor is a fact in a vernier machine but not inherently caused by a high armature inductance. The poor power factor can be overcome by increasing useful flux from PM, which is the desired method used in this article. In addition, a low power factor also occurs in series of high pole number variable-reluctance machines such as the magnetic geared machine and the transverse-flux PM machine typically with a value about 0.35-0.55 [4],[7]-[8]. Similar methods for the power factor improvement can also be researched in these classes of machine.

Various types of double excitation or complex magnetized PM vernier machines have been designed to increase the torque density and utilize the limited space in the permanent magnet machine effectively. However, an advanced topology or method to effectively improve both torque density and power factor of a PM vernier machine continues to be desired and is the main objective of this article. In particular, an analysis is carried out using a spoke array magnet and an unaligned dual stator placement. The spoke array usefully generates a high flux density in airgap. The dual stator design introduces an effect on flux focusing to drive the flux to flow over the entire dual air gap machine and relatively decrease the leakage flux. This improved topology contributes to the superiority of the PM vernier machine for competing with high quality PM machines or other variable-reluctance machines for a low speed, high torque application.

To compare the machines conveniently, two topologies with same overall volume and same stator have been investigated:

- A normal 3-phase dual-stator surface PMVM (DS-SPMVM) as in Fig.1, which has two-layer magnets mounted on the rotor surface and two tooth-tooth aligned stators.
- A proposed 3-phase dual-stator interior PMVM (DS-IPMVM) as in Fig. 2,

which has spoke array magnets perpendicular to the airgaps and two half-slot-pitch shifted stators.

Both prototypes have been designed with 17 magnet pole pairs in rotor, 18 open slots in each stator and one pole pair 3-phase concentrated windings. The specifications of both models are tabulated in Table I. The operation principle and theoretical analysis of the no-load magnetic field in the proposed DS-IPMVM has been investigated and verified by a two dimensional finite element method (2D FEM). The flux line distribution and the equivalent magnetic circuit of both machines are given. The transient performance of both machines were simulated for comparison, where the FEM models take the saturation effect and core loss into account. Finally, the slot optimization design of the proposed machine is constructed for maximum torque density and power factor.

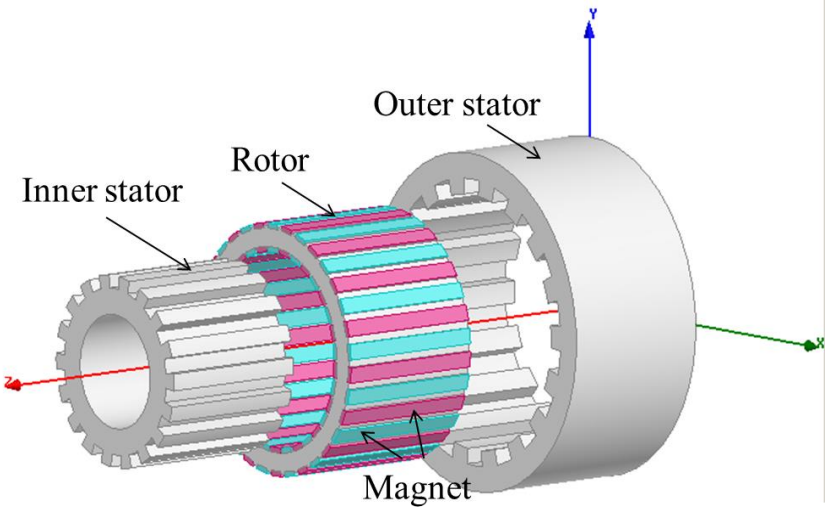

Fig. 1 Topology of a normal DS-SPMVM.

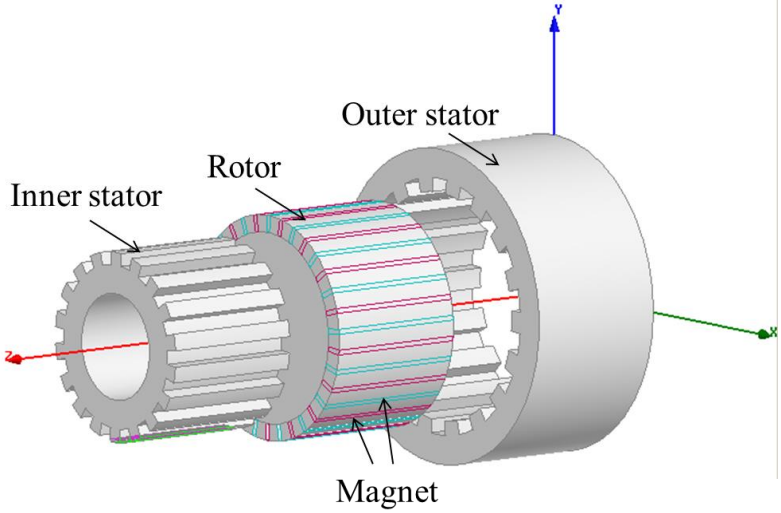

Fig. 2 Topology of a proposed DS-IPMVM.

TABLE I
SPECIFICATIONS OF BOTH MODELS

Items		Unit	DS-SPMVM	DS-IPMVM
Outer stator	Outer diameter	mm	130	
	Inner diameter	mm	98	94
Inner stator	Outer diameter	mm	74	78
	Inner diameter	mm	44	
Outer stator winding turns/slot		-	26	
Inner stator winding turns/slot		-	18	
Outer airgap length		mm	0.6	
Inner airgap length		mm	0.4	
Stack length		mm	60	
No. of stator slots		-	18*2	
No. of rotor pole-pairs		-	17*2	17
Core volume		cm^3	528	570
PM volume		cm^3	49	28
Remanence of PM (NdFeB)		T	1.23	

2. Magnetic field analysis and machine performance comparison

2.1 Proposed machine

The proposed configuration of DS-IPMVM supplies a flux-focusing design using spoke-arranged magnets to increase the useful magnet flux and decrease the flux leakage between adjacent PMs. As shown in Fig. 3, the rotor pole drives flux across both outer/inner airgap with half slot pitch shifted dual stators. The flux circumferentially travels in the one stator core, back across the air gap into the rotor and flows into another air gap into the other stator core. The flux lines in two specified relative positions are shown in Fig. 3 (a) and (b). This flux-focusing designed topology can be applied in either a radial flux or an axial flux arrangement. The length of the magnet can be designed to obtain the desired flux focusing conveniently. Since the field frequency is the ratio of magnet poles/armature pole times the armature frequency, the reactance is also highly increased, which can easily result a poor power factor.

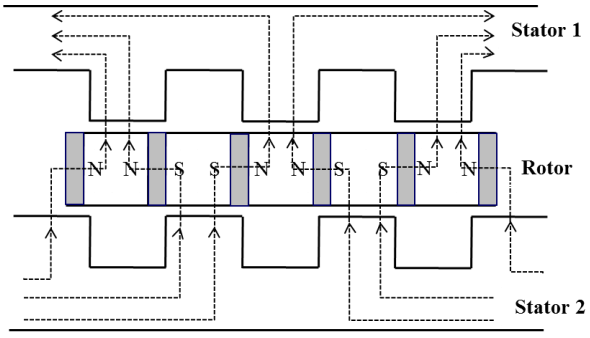

(a) Machine topology

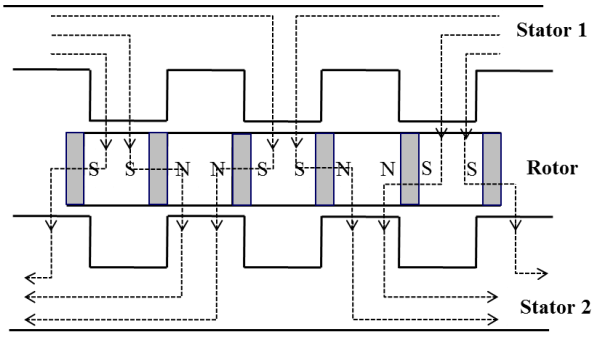

(b) Machine topology rotated by half of magnet pole pitch

Fig. 3. Magnet flux loop in DS-IPMVM.

The high-torque low-speed desirable feature is brought out by a magnetic gearing effect due to its toothed-pole structure. If p, Z_s and Z_r are the numbers of stator winding pole pairs, stator teeth and rotor pole pair respectively in a PMVM, there exists a rule in which

$$Z_r = Z_s \pm p \tag{1}$$

This principle has been explained by previous authors with various expressions to produce steady torque [3]-[6]. While the number of stator winding pole and rotor poles is unequal, the machine still achieves smooth torque by synchronizing the space harmonics of the stator magneto-motive force (MMF) with the rotor magnets MMF. As the rotor rotates, the machine produces a rotor magnet MMF with Z_r pole pairs in the airgap. It is modulated by gap permeance due to the flux modulation effect from the open stator teeth. Thus the magnetic flux density of the gap by magnet contains the fundamental wave p pole pairs of the same order with stator MMF as well as other harmonic components. The stator armature MMF produces a second rotating field with p pole pairs and both interact to produce the synchronous reaction torque. In addition, the slot harmonic component in vernier machine also contributes to production of useful torque. This phenomenon is the reason why it has an increase torque compared with the normal PM machine.

Magnetic field of the proposed DS-IPMVM can be analyzed by its unit block, called an elementary domain [3] which contains one tooth, one slot and one magnet pole pair as in Fig. 4. Here, reference axis is selected as the center line of a slot, θ_m and θ are the rotor position and mechanical angle on the stator, respectively.

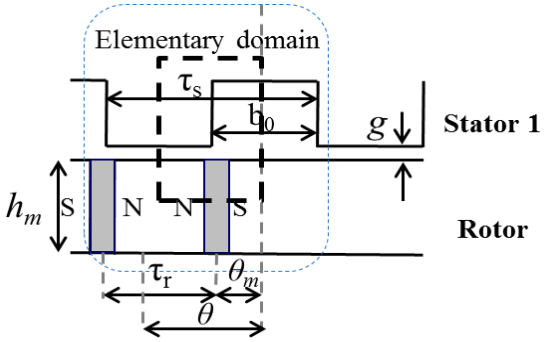

Fig. 4. Elementary domain in half of the proposed DS-IPMVM.

The permeance coefficient P is defined as the permeance per unit area to the radial direction in the airgap and expressed as

$$P(\theta) = P_0 + (-1)^j \sum_{m=1}^{\infty} P_m \cos(mZ_s\theta) \tag{2}$$

$$P_0 = \frac{\mu_0}{g_e} = \frac{\mu_0}{k_{cs}k_{cr}g} k_{c0} \tag{3}$$

$$P_1 = \frac{2\mu_0\beta}{\pi g} \sin(1.6\pi \frac{b_0}{\tau_s}) \frac{1}{1-1.6^2(\frac{b_0}{\tau_s})^2} \tag{4}$$

The quantity P_0 is an average air gap permeance which utilizes both of the stator Carter coefficient k_{cs} and rotor Carter coefficient k_{cr}. P_m is the amplitude of the *mth* harmonic, and j is the number of slot shifts of the short pitch windings. k_{c0} is a coefficient related to airgap and stator slot [9], [10].

Using Ampere's law in the dotted path of Fig. 4 and ignoring the MMF in the core to obtain the fundamental amplitude of airgap MMF F_{g1} is shown in (5)-(7). The relative permeability of the permanent magnet is same as the air, so the permeance of the air area F_{gapm} which contains permanent magnet should also be considered and given by

$$F_{gap1} + F_{gap2} + F_{gapm} + F_m = 0 \tag{5}$$

$$F_m = \pm \frac{B_r g_m}{\mu_m} \tag{6}$$

$$F_{g1} = \frac{4}{\pi} F_g = \frac{4}{\pi} \frac{\frac{B_r g_m}{\mu_m}}{2 + \frac{P_0 g_m}{2h_m\mu_0}\tau_r} \tag{7}$$

$$F_g(\theta) = F_{g1}[\cos(Z_r(\theta - \theta_m)) + \sum_{n=3,odd}^{\infty} \frac{1}{n} \cos(nZ_r(\theta - \theta_m))] \tag{8}$$

where B_r and μ_m are the residual flux density and permeability of the magnet, respectively. Detailed parameter definitions are explained in Fig. 4.

The flux density is produced by the MMF and permeance, so when only consider the major order of m = 0, 1 and n = 1 components, the no load flux density due to PM in the airgap is expressed as below with a frequency of p,

$$\begin{aligned} B_{PM} &\approx B_{PM0}\cos(Z_r(\theta - \theta_m)) + (-1)^j B_{PM1}\cos((Z_r - Z_s)\theta - Z_r\theta_m) \\ &\approx F_{g1}P_0\cos(Z_r(\theta - \theta_m)) + (-1)^j \frac{F_{g1}P_1}{2}\cos((Z_r - Z_s)\theta - Z_r\theta_m) \end{aligned} \tag{9}$$

The airgap flux density value is calculated and verified by the FEM result as in Table II. The slot harmonic component is important for the machine torque production [1]-[6], [11]. Thus, the theoretical analysis result of flux density is some lower than the FEM result, which only contains the fundamental and 1*st* order components. Non-uniform airgap in both sides causes the potential to be

uneven on the surface of spoke-array magnet too, which also causes error between two methods.

TABLE II
COMPARISON OF THE RESULTS BY 2D FEM AND THEORETICAL ANALYSIS

Item	Unit	DS-IPMVM	
		2D FEM	Theoretical analysis
Inner airgap flux density	T	0.57	0.55
Outer airgap flux density	T	0.76	0.71

2.2 Performance comparison

The configurations, no-load flux line distributions and equivalent magnetic circuits (EMC) of both models are shown in Fig. 5 and 6 respectively, where F_a is the stator armature MMF, F_m is the PM MMF, Λ_m is the PM permeance, Λ_r is the rotor permeance, Λ_σ is the leakage permeance, Λ_δ is the main permeance including the air gap and stator core, Φ_σ is the leakage flux, Φ_δ is the main magnetic flux and Φ_m is the PM flux [12]. Both models adopt the open slot type and the drum winding with the coil wound around each stator yoke. Windings of two stators can be connected in series and also can be controlled separately for various operation demands.

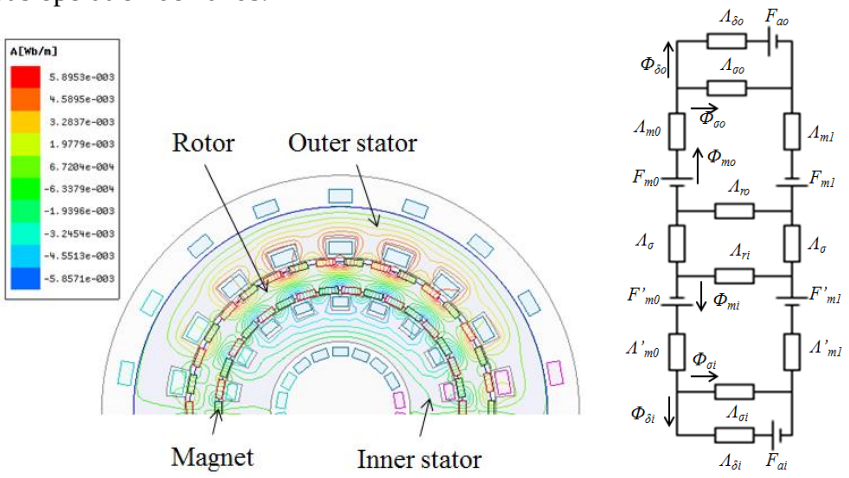

Fig. 5. No-load flux line distribution and EMC in DS-SPMVM.

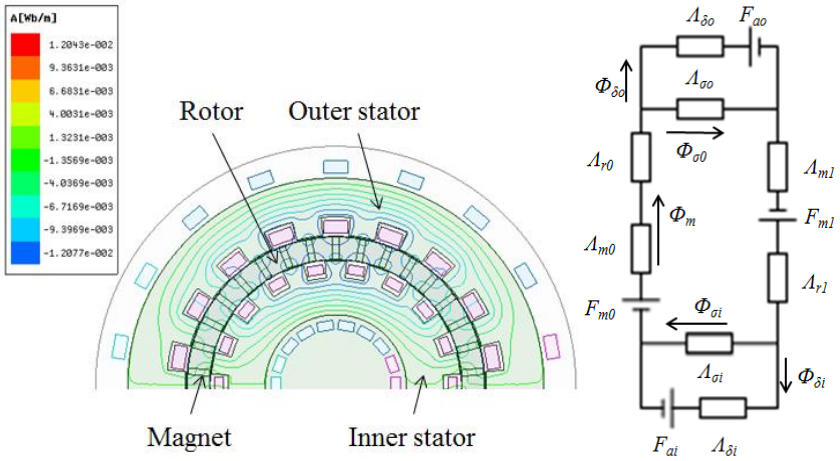

Fig. 6. No-load flux line distribution and EMC in DS-IPMVM.

In order to manufacture the machine easily, the magnet can be made with a rectangular shape and inserted half into the rotor core in the DS-SPMVM, which leads to higher cogging torque due to the unbalanced tooth-slot flux path. In the no-load condition, Back-EMF is simulated at rated speed as in Fig. 7 and versus a speed region in Fig. 8, where different slops are caused by different number of turns per phase in two inner and outer stator windings. Cogging torque (peak to peak value) of two machines is shown as in Fig. 9 at rated speed.

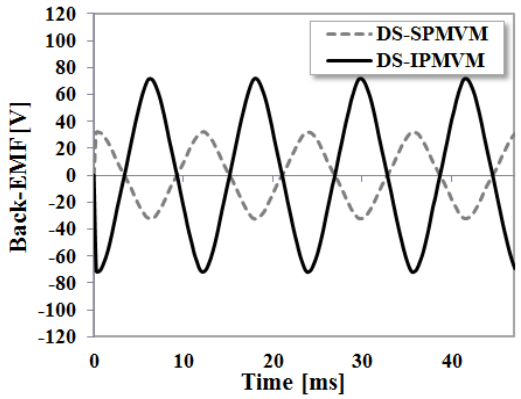

Fig. 7. Phase back-EMF waveform in the outer stator at 300 rpm.

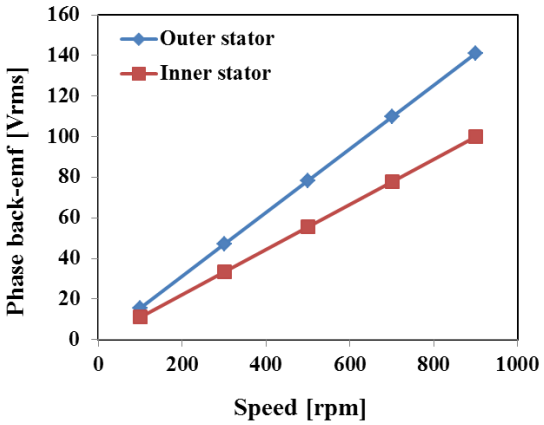

Fig. 8. Back-EMF versus rotor speed in the proposed DS-IPMVM.

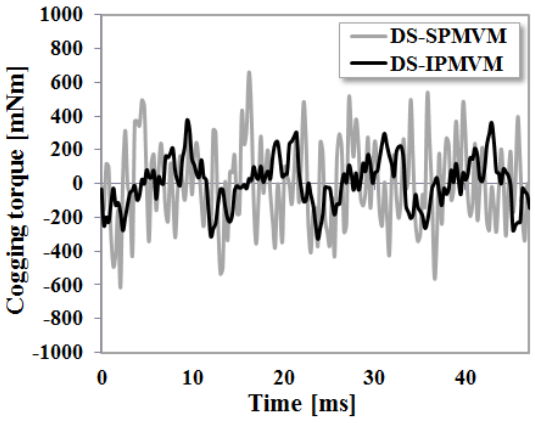

Fig. 9. Cogging torque waveforms at 300 rpm.

Fig. 10 shows the no-load flux density waveforms in the inner airgap and outer airgap respectively at the same rotor position. Either the waveforms in (a) or (b) contain the sinusoidal fundamental component with a same trend and the specific space harmonics in the airgap occurs because of that magnetic gearing effect and the tooth flux modulation function, where the teeth have the same effect as the ferromagnetic pieces in a magnetic gear [13], [14]. Flux density in the inner airgap is higher than that in the outer airgap due to a shorter airgap length design.

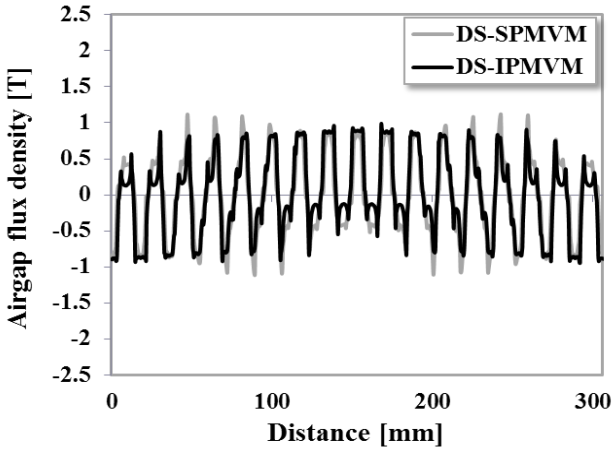

(a) In the outer airgap

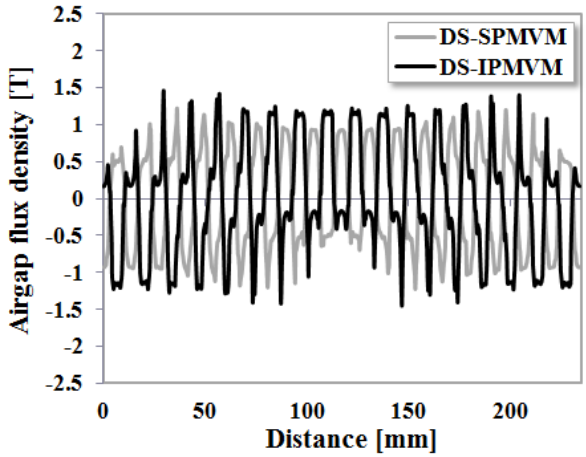

(b) In the inner airgap

Fig. 10. Waveforms of no-load flux density in each airgap at 300 rpm.

The steady electromagnetic torque versus the phase advanced angle is compared in Fig. 11 with 4.4 Arms rated current at 300 rpm, where the phase advanced angle is defined as the phase angle between phase current and back-emf. Fig. 12 shows the flux density distribution, where the large PM leakage flux in DS-SPMVM can easily cause rotor core saturation without any magnetic separation device inside. However, exact same dimensions of stator and rotor cores in both machines will lead to flux density highly increasing up to saturation in proposed DS-IPMVM. Thus, the stator yoke thickness in the DS-IPMVM has 2 mm increase to avoid the core saturation. In Fig. 12 (b), the magnet flux focusing designed DS-IPMVM can utilize the core portion effectively, while the coreloss is increased due to higher flux density and more steel core utilization.

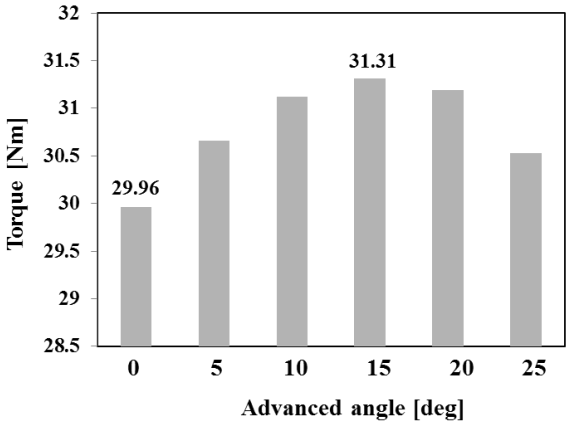

Fig. 11. Electromagnetic torque versus phase advance angle in the proposed DS-IPMVM.

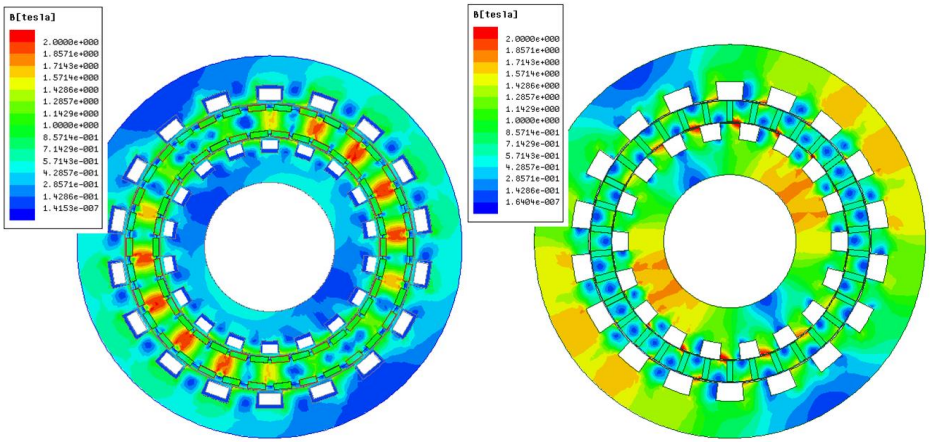

(a) DS-SPMVM (b) DS-IPMVM

Fig. 12. Flux density distribution with armature excitation.

TABLE III
ANALYSIS RESULTS USING FEM

Items	Unit	DS-SPMVM	DS-IPMVM
Outer back-EMF	V_{rms}	21.3	48
Inner back-EMF	V_{rms}	12.6	34
Cogging torque	Nm	1.3	0.9
Core loss	W	10.4	31.5
Power factor	-	0.66/0.69	0.76/0.87
Torque	Nm	11.8	30
Torque density	Nm/l	15	38
Efficiency	%	89.1	93.3

Table III sums up the main performance by 2D FEM in both models. The solutions with load are simulated with zero phase advance angle. Power factors here are separately measured in the two groups of stator windings. The torque density in the proposed DS-IPMVM is 2.5 times that of the DS-SPMVM, which represents the ratio of torque to the machine overall volume. Thus, the high

torque leads to 4.2% higher efficiency in the DS-IPMVM even though the core loss is 3 times that of the DS-SPMVM.

3. Tooth optimization design in the proposed DS-IPMVM

Stator tooth in a vernier machine is in charge of the space flux modulation. Stator slot pitch affects the Carte's coefficient in the airgap permeance calculation. Thus, the tooth optimization design is a good choice to obtain an even larger torque density and a higher power factor. The optimal design process is constructed as in Fig. 13 and also needs to arrange the flux density reasonable in the core. In this optimum design, the rotor topology, the stator dimensions, winding and slot pole pair number have no change.

During the optimal design process, Latin Hypercube Sampling (LHS) was selected to disperse sampling points and also to not overlap sampling points [15]. The LHS was applied as a method of the design of experiment (DOE) and the Kriging model was used to approximate the objective and constraints functions. A genetic algorithm (GA) was utilized as the optimization algorithm and the optimized result by GA is finally verified by FEM. Fig. 14 supplies the torque variation versus the variable range of X_1 (tooth width to pitch) and X_2 (tooth height to pitch), which has an optimum result in the condition of X_1=0.37, X_2=0.26 with the slot pitch as 0.63.

Objective function
- Maximum torque and power factor

Constraint
- Output torque>30 Nm
- PF >0.81

Variable candidates
- X_1 – tooth width to tooth pitch ratio
- X_2 – tooth height to tooth pitch ratio

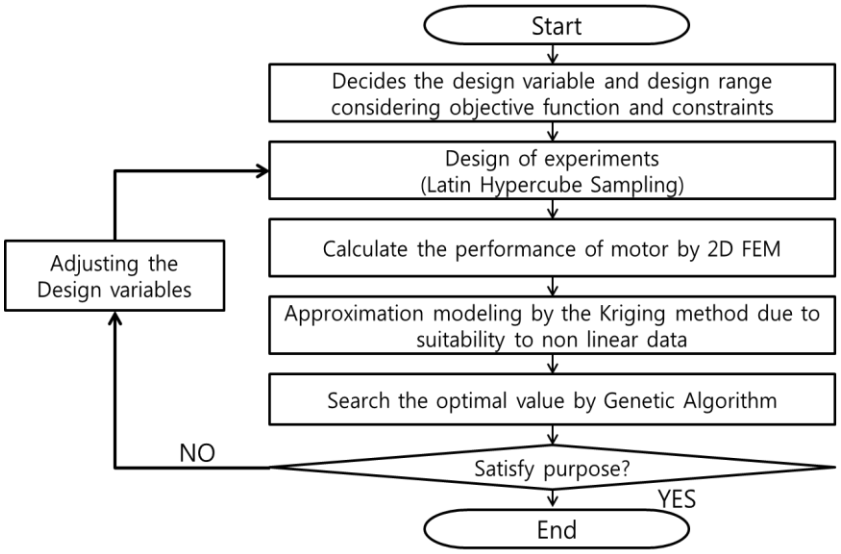

Fig. 13. Flowchart of optimization design process.

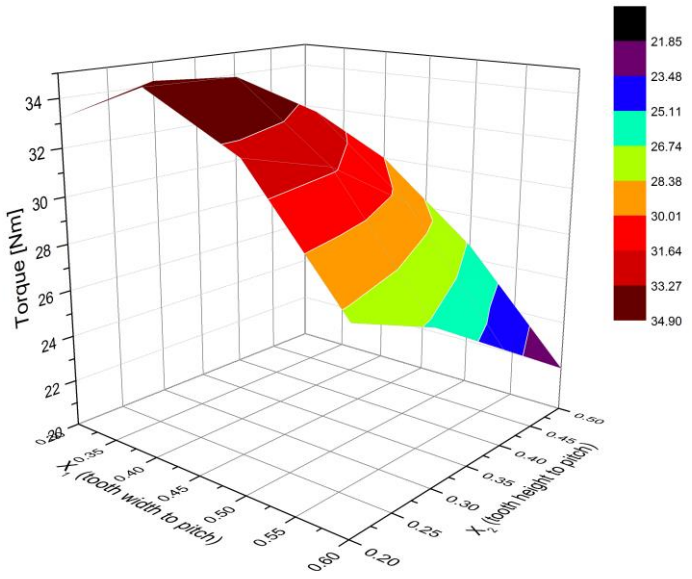

Fig. 14. Torque versus tooth dimensions.

TABLE IV
ANALYSIS RESULTS USING FEM

Items	Unit	Initial model	Optimal model	
		FEM		Optimal Algorithm
X_1	-	0.5	0.368	
X_2	-	0.35	0.256	
Core volume	cm^3	556	331	
Core loss	W	31.5	29.5	-
Power factor (avg.)	-	0.81	0.868	0.871
Torque	Nm	30	35.27	35.34
Torque density	Nm/l	38	44	-
Efficiency	%	93.3	94	-

4. Conclusion

An improved topology, the DS-IPMVM has been proposed in this article, where the magnets are perpendicularly aligned to the air gap as a flux focusing design and two stators are half-slot pitch shifted. This design greatly improves the useful magnet flux compared with the normal DS-SPMVM. The simulation results using 2D FEM show the proposed topology achieves higher torque density, higher flux density, higher power factor and lower cogging torque with less magnet volume compared to the conventional DS-SPMVM. In addition, the proposed machine can obtain a larger electromagnetic torque by use of a suitable current vector control.

Research on a full theoretical analysis including expressions for torque and

power factor of the proposed dual-stator spoke-array magnet vernier machine for accurate design is under development. In addition, it appears that the winding layout and the magnet dimensions can be further optimized for improvement in characteristics such as high torque, high power factor, less copper loss, high efficiency.

References

[1] A. Ishizaki, T. Tanaka, K. Takasaki and S. Nishikata, "Theory and optimum design of PM vernier motor," *in Proc. of IEEE ICEMD'95*, 1995, pp. 208-212.

[2] C. H. Lee, "Vernier motor and its design," IEEE Transactions on Power Apparatus and Systems, vol. 82, no. 66, 1963, pp. 343-349.

[3] A. Toba and T. A. Lipo, "Generic torque-maximizing design methodology of surface permanent–magnet vernier machine," *IEEE Trans. on Industry Applications*, vol. 36, no. 6, pp. 1539-1546, Nov. /Dec. 2000.

[4] A. Toba and T. A. Lipo, "Novel dual-excitation permanent magnet vernier machine," *in Proc. Conf. Rec. IEEE 34th IAS Annual Meeting*, 1999, pp. 2539-2544.

[5] S. L. Ho, Shuangxia Niu and W. N. Fu, "Design and comparison of vernier permanent magnet machines," *IEEE Trans. Magn.*, vol. 47, no. 10, pp. 3280-3283, Oct. 2011.

[6] F. Zhao, T. A. Lipo and B. I. Kwon, "Magnet flux focusing design of double stator permanent magnet vernier machine," *Proc. of 2013 Conference on the Computation of Electromagnetic Fields (COMPUMAG 2013)*, July 2013.

[7] M. R. Harris, G. H. Pajooman, and S. M. Abu Sharkh, "The problem of power factor in VRPM (transverse-flux) machines," *in Proc. of IEEE ICEMD'97*, No. 444, pp. 386-390, Sep. 1997.

[8] Linni Jian, K. T. Chau, and J. Z. Jiang, "A magnetic-geared outer-rotor permanent-magnet brushless machine for wind power generation*." Industry Applications, IEEE Transactions on*, vol. 45, no. 3 pp. 954-962, 2009.

[9] Z. Q. Zhu, D. Howe, "Instantaneous magnetic field distribution in brushless permanent magnet DC motors. III. Effect of stator slotting," *IEEE Trans. Magn.*, vol. 29, no. 1, pp.143-151, Jan. 1993.

[10] T. A. Lipo, *Introduction to AC machine design*, (book) University of Wisconsin-WEMPEC, 3rd ed., 2007, pp. 95-101.

[11] H. Kakihata, Y. Katoka, and M. Takayma, "Design of surface permanent magnet-type vernier motor," *in Proc. ICEMS*, 2012, Sapporo, pp. 1-6.

[12] Shuangxia Niu, K. T. Chau and Chuang Yu, "Quantitative comparison of double-stator and traditional permanent magnet brushless machines," *Journal of Applied Physics*, vol. 105, no.7, pp. 07F105-07F105, 2009.

[13] K. Atallah and D. Howe, "A novel high-performance magnetic gear," *IEEE Trans. Magn.*, vol. 37, no. 4, pp: 2844-2846, 2001.

[14] R. Qu, D. Li, J. Wang, "Relationship between magnetic gears and vernier machines," *in Proc. ICEMS*, 2011,Bejing, pp. 1–6.

[15] J. B. Kim, et al., "Optimization of Two-Phase In-Wheel IPMSM for Wide Speed Range by Using the Kriging Model Based on Latin Hypercube Sampling", *IEEE Trans. Magns.*, vol. 47, no. 5, pp. 1078-1081, May 2011.